NASA
Technical Memorandum 101460

AVSCOM
Technical Report 88-C-034

Lubricant Jet Flow Phenomena in Spur and Helical Gears with Modified Addendums—for Radially Directed Individual Jets

Lee S. Akin
California State University
Long Beach, California

and

Dennis P. Townsend
Lewis Research Center
Cleveland, Ohio

Prepared for the
Fifth International Power Transmission and Gearing Conference
sponsored by the American Society of Mechanical Engineering
Chicago, Illinois, April 25–27, 1989

NASA

US ARMY
AVIATION
SYSTEMS COMMAND

LUBRICANT JET FLOW PHENOMENA IN SPUR AND HELICAL GEARS WITH MODIFIED ADDENDUMS - FOR RADIALLY DIRECTED INDIVIDUAL JETS

Lee S. Akin
California State University
Long Beach, California 90815

and

Dennis P. Townsend
National Aeronautics and Space Administration
Lewis Research Center
Cleveland, Ohio 44135

E-4533

ABSTRACT

This paper develops the mathematical relations for the "Virtual Kinematic Model" as an improvement over the vectorial model developed earlier. The model solution described herein provides the most energy efficient means of cooling gears - that is, it requires the least pressure or pumping power to distribute the coolant on the tooth surface. Further, this nozzle orientation allows impingement to the root of the tooth if needed and provides the most cooling control when compared to into-mesh or out-of-mesh cooling.

NOMENCLATURE

a	addendum of tooth
d_i	impingement depth
d_x	uncorrected impingement depth in origin plane
ev	of Θ = sec ϕ = evolvent function of Θ
N	number of teeth in gear
n	rotational speed
P_d	diametrical pitch
P_n	normal diametrial pitch
P_t	transverse diametrial pitch
R	standard pitch radius
R_b	base radius of gear
R_{bv}	base radius of virtual involute
R_i	radius at impingement point
R_{or}	operational outside radius (for modified addendum)
R_o	standard outside radius
R_t	transverse pitch radius
R_x	uncorrected radius at impingement point (see Fig. 3)
t	arbitrary flight time
t_f	jet stream flight time at impingement
t_w	time to rotate through angle, Θ_w
V_g	linear pitch line velocity of gear
V_j	jet velocity
α	jet inclination angle
Δa	addendum modification
δ_i	dimensionless impingement depth $\frac{d_i P_d}{2}$
ε_{iv}	virtual roll angle at impingement point
ε_{ov}	virtual roll angle to outside diameter
Θ_a	vectorial angle of involute between point i and 0 (Fig. 2)
Θ_i	involute of ϕ_i = involute function at impingement point
Θ_{iv}	virtual vectoral angle to impingement point
Θ_{ov}	virtual vectoral angle to outside diameter
Θ_r	angle across tooth space at base circle
Θ_w	total vectoral angle at impingement point
ν_j	dimensionless jet velocity V_j/V_g
ρ_b	dimensionless base circle radius
ρ_i	dimensionless impingement radius

ρ_{or} dimensionless outside radius

ρ_t dimensionless transverse pitch radius

ϕ pressure angle at pitch radius

ϕ_i pressure angle at impingement point

ϕ_{iv} pressure angle of virtual involute at impingement point

ϕ_n normal pressure angle

ϕ_o pressure angle at outside radius

ϕ_{ov} pressure angle of virtual involute at outside diameter

ϕ_t transverse pressure angle

ψ helical angle

ω_g gear angular velocity

ω_j virtural jet angular velocity

INTRODUCTION

Cooling of lightweight high speed gears via the lubricating oil supply provided to the gearbox continues to be one of the most difficult areas in the high performance mechanical power transmission design process. Since the cooling process is controlled by oil jet orientation and by the jet velocity relative to the pitch line velocity (PLV), these authors have considered the development of a fundamental understanding of the oil jet primary impingement phenomena as essential to understanding how the gear tooth cooling process works. In the early 1970's when this work was started, a "vectorial model" was used to describe the radial jet flow phenomena, (Akin, 1975), which compared reasonably well with the experimental data, (Akin, 1975), especially at pressures above approximately 140 kPa (20 psi). Models were also developed for into mesh (Akin, 1983) and for out of mesh (Akin, 1985) to determine the oil jet impingement depths for these conditions. The into mesh and out of mesh models indicate the oil jet impingement depths were limited and therefore maximum cooling could not be obtained using this approach.

The "Virtual Kinematic Model" was first mentioned by Townsend in 1980, but the full mathematical development of this model has not been published until now. This model has been generalized to include spur or helical gears with standard AGMA proportions as well as long or short addendums. Further, parametric limitations have been formulated to allow the gear analyst to know he is specifying his problem where a solution is possible. Also, the dimensionless parameter development has been provided to allow the gear engineer to examine a wide range of generalized solutions easily and to expose the limits mentioned above.

KINEMATIC SOLUTION FOR MODIFIED SPUR GEARS

The jet stream flight time starts ($t = 0$) at position "1" at the intersection of the top land and trailing profile of the leading tooth, as shown in Fig. 1. Then the terminal end of the jet passes through the tooth space where it impinges at "i" on the leading profile of the trailing tooth at radius R_i after time ($t = t_f$). From inspection of Fig. 1, it can be seen that the radius of impingement is:

$$R_i = R_o - V_j t_f \tag{1}$$

where V_j is the jet velocity. The time of flight of the oil jet through the tooth space is:

$$t_f = \frac{R_o - R_i}{V_j} = \frac{d_i}{V_j} \quad \text{sec} \tag{2}$$

The gear must rotate through the angle θ_w in the same time it takes the oil jet to travel through the tooth space to a depth of $d_i = V_j t_f$ and impinge at R_i. From Fig. 1 we see that $\theta_w = \theta_o + \theta_r + \theta_i$. The components of θ_w are developed below.

The pressure angle, ϕ_i, at the depth of impingement, d_i is:

$$\phi_i = \cos^{-1}\left(\frac{R_b}{R_i}\right) \text{ and } \tan\phi_i = \left[\frac{R_i^2}{R_b^2} - 1\right]^{1/2} \tag{3}$$

where

R_b is the gear base radius

$$R_i = R_o - d_i$$

so that $\theta_i = \text{inv}\,\phi_i = \tan\phi_i - \phi_i$.

Also, the angle across the tooth space at the gear base circle is:

$$\theta_r = \frac{\pi}{N} - 2\,\text{inv}\,\phi = \frac{\pi}{N} - 2(\tan\phi - \phi) \tag{4}$$

where $\phi = \cos^{-1}(R_b/R)$ is the pressure angle at the standard pitch circle R. Further, the pressure angle at the outside radius R_o is:

$$\phi_o = \cos^{-1}\left(\frac{R_b}{R_o}\right) \text{ and } \tan\phi_o = \left[\frac{R_o^2}{R_b^2} - 1\right]^{1/2} \tag{5}$$

so that

$$\theta_o = \text{inv}\,\phi_o = \tan\phi_o - \phi_o$$

and thus

$\theta_w = \theta_o + \theta_r + \theta_i$ as stated earlier, so that the time it takes the gear to rotate through θ_w is

$$t_w = \frac{\theta_w}{\omega_g} = \frac{30\,\theta_w}{\pi n} \text{ sec;} \tag{6}$$

where n = rev/min.

Equating the times of flight t_i and rotation t_w:

$$\frac{d_i}{V_j} = \frac{30\,\theta_w}{\pi n} \quad \text{or} \quad \frac{R_o - R_i}{V_j} = \frac{\theta_w}{\omega_g} \tag{7}$$

If d_i is given, then the required V_j can be found explicitly as

$$V_j = \frac{\omega_g d_i}{\theta_w} = \frac{\pi d_i n}{30\,\theta_w} \qquad (8)$$

note, that d_i is a function of $\phi_i (d_i = f_n(\phi_i))$

If V_j is given and the resulting d_i or R_i is desired, we must iterate until R_i, as $fn(\phi_i, V_j)$, is satisfied. In dimensionless form, where: $\nu_j = V_j/V_g$ and $\delta_i = d_i P_d/2$

$$\nu_j = \frac{d_i}{R_o \theta_w} = \frac{4\delta_i}{[(N+2)\theta_w]} \qquad (9)$$

GEARS WITH MODIFIED ADDENDUMS AND AN OIL JET DIRECTED AT AN ARBITRARY INCLINATION ANGLE α FROM THE GEAR CENTER

A more general solution can be provided to this problem if we assume that the jet is pointed away from the line through center of the gear by an arbitrary angle "α" as shown in Fig. 2. This angle is defined to be positive in magnitude when pointed in the direction of ω_g as shown in Fig. 2. Modified addendum lengths or center distances are accommodated by the use of the parameter $\Delta R_o = \Delta N_g/2P_n = \Delta a$, so that $R_{or} = R_o + \Delta a$. Obviously when $\Delta a = 0$, $R_o = R_{or}$. In this paper we will generalize and use Δa, R_o, and R_{or} in all equations.

For helical gears we let: $R_t = N(2P_n \cos \psi)$, so that, $R_o = R_t + a$ and $R_{or} = R_t + a + \Delta a$, where $P_t = P_n \cos \psi$ and the subscript t refers to the transverse plane (normal to gear axis.) This problem has been formulated by assuming that the jet terminal end (or head) follows a trajectory in mesh with a "virtual involute" as shown in Fig. 2. The virtual involute is: defined by the radius of the base circle R_{bv}, where

$$R_{bv} = R_{or} \sin \alpha, \quad V_j = \omega_j R_{bv}, \quad \text{or} \quad \omega_j = \frac{V_j}{R_{or} \sin \alpha} \qquad (10)$$

As can be seen by inspection of Fig. 2, "ω_j" is the theoretical angular velocity of the virtual jet involute that produces the proper locus for the terminal end of the jet stream line at the actual jet velocity V_J, subsequent to passing the point 1 at $t = 0$. The virtual involute is used to develop the mathematical relationships needed to formulate the time of flight to impingement of the jet stream on the trailing tooth profile at R_i when the gear angular velocity is ω_g. Note that in general $\omega_g \neq \omega_j$ since the virtual base circle is not fixed on the gear blank (or wheel).

The writer has selected the virtual involute generalized roll angle ε_v as the parameter to interrelate the virtual involute for the jet stream with the rotating gear geometry. Thus the virtual roll angle ε_{ov} at the gear outside diameter can be calculated from the fundamental relationship (see Fig. 2):

$R_{bv}\,\varepsilon_{ov} = R_{or} \cos \alpha$, so that ε_{ov}

$$= \frac{R_{or} \cos \alpha}{R_{bv}} = \frac{R_{or} \cos \alpha}{R_{or} \sin \alpha} = \frac{1}{\tan \alpha} = \cot \alpha \quad (0 < \alpha < \tfrac{\pi}{2}) \qquad (11)$$

From here we can develop the remainder of the virtual involute functions including θ_{ov} and ϕ_{ov} as follows (see Fig. 2):

$\varepsilon_{ov} = (ev^2\theta - 1)^{1/2}$ or $ev\,\theta = (\varepsilon_{ov}^2 + 1)^{1/2}$ where by definition (Vogel, 1945):

$ev\,\theta = R_{or}/R_{bv}$, so that $\varepsilon_{ov} = [(R_{or}/R_{bv})^2 - 1]^{1/2}$ avoids the use of α functions. The virtual vertorial angle or polar angle θ_{ov} at the O.D. is:

$\theta_{ov} = [R_{or}/R_{bv})^2 - 1]^{1/2} - \tan^{-1}[(R_{or}/R_{bv})^2 - 1]^{1/2}$ (rad.) and the virtual pressure angle ϕ_{ov} is obtained from:

$$\phi_{ov} = inv^{-1}\theta_{ov} = sec^{-1}(ev\,\theta_{ov}) = \cos^{-1}(R_{bv}/R_{or}). \qquad (12)$$

From the above we get $\varepsilon_{ov} = \theta_{ov} + \phi_{ov}$ as a check. Also, $\alpha = \alpha_{ov} = \pi/2 - \phi_{ov}$ (rad) as a check)

$$\varepsilon_{ov} = \frac{R_{or} \cos \alpha}{R_{bv}} = \cot \alpha \quad (0 < \alpha < \tfrac{\pi}{2}) \qquad (13)$$

The virtual roll angle ε_{iv} at the impingement diameter is developed as follows:

$$\varepsilon_{o-i} = \varepsilon_{ov} - \varepsilon_{iv} = \omega_j t_f = \frac{V_j t_f}{R_o \sin \alpha} \qquad (14)$$

so that $\varepsilon_i(t_f) = \varepsilon_{ov} - \omega_j t_f = (R_{or} \cos \alpha - V_j t_f)/(R_{or} \sin \alpha) = \cot \alpha - V_j t_f/(R_{or} \sin \alpha)$.

Note from Fig. 2 that $V_j t_f = d_i/\cos \alpha$, thus when V_j and/or t_f are unknown:

$$\varepsilon_{iv}(d_i) = \frac{R_{or} \cos \alpha - \frac{d_i}{\cos \alpha}}{R_{or} \sin \alpha} = \cot \alpha - \frac{d_i}{R_{or} \sin \alpha \cos \alpha}$$

and $\varepsilon_{o-i} = \varepsilon_{ov} - \varepsilon_{iv}$

$$= \cot \alpha - \cot \alpha + \frac{d_i}{R_{or} \sin \alpha \cos \alpha} = \frac{2d_i}{R_{or} \sin 2\alpha} \qquad (15)$$

Again the other virtual involute functions at the impingement diameter are; starting with the vectoral angle:

$$\theta_{iv} = \left[\frac{(R_{or} - d_i)^2}{R_{bv}^2} - 1\right]^{1/2} - \tan^{-1}\left[\frac{(R_{or} - d_i)^2}{R_{bv}^2} - 1\right]^{1/2} \quad \text{(rad.)} \qquad (16)$$

and the virtual pressure angle ϕ_{iv} at R_i:

$$\phi_{iv} = \cos^{-1}\left[\frac{R_{bv}}{R_{or} - d_i}\right] \qquad (17)$$

Further noting that

$$\varepsilon_{iv} = \left[\frac{(R_{or} - d_i)^2}{R_{bv}^2} - 1\right]^{1/2} = \phi_{iv} + \theta_{iv} \quad \text{as a check, and} \qquad (18)$$

$$\alpha_{iv} = \frac{\pi}{2} - \phi_{iv}(\text{rad.}) \quad \text{and} \quad R_i = R_{bv}(\varepsilon_{iv}^2 + 1)^{1/2}$$

as a check. Thus the time of flight can be checked from:

$$t_f = \frac{\varepsilon_{o-i}}{\omega_j} = \frac{d_i}{R_{or} \sin\alpha \cos\alpha[V_j/(R_{or} \sin\alpha)]}$$

$$= \frac{d_i}{V_j \cos\alpha} \quad (\text{sec}) \qquad (19)$$

where

$$d_i = (R_o + \Delta a) - R_i = R_{or} - R_i$$

Theoretically, the virtual involute is a dummy device for mathematically describing the time motion of the terminal end of the jet stream line. As such, the jet stream line is the line of action between the virtual involute and the oil jet. Thus the coincident points "i" at radius r_i on the virtual involute (v.i.) and R_i on the gear tooth (g.t.) define the point of oil impingement at time t_f (v.i.) = t_w (g.t.). This coincident instant in time is the result of the simultaneous motions of the (v.i.) and (g.t.) from time $t = 0$ when the (v.i.) is at its outer position 2 at the virtual base circle (Fig. 2) while the trailing edge of the leading gear tooth is at position "0" where the jet line crosses the O.D. and the (v.i.) is such that the rotation of the (v.i.) at ω_g without the relative rotation of $(\omega_j - \omega_g)$ through time t_w would place the (v.i.) origin at position 3 at the virtual base circle. Thus the (v.i.) is preceived to rotate faster than ω_j by the amount $(\omega_j - \omega_g)$ such that it rotates at $\omega_g + (\omega_j - \omega_g) = \omega_j$ in keeping with the jet velocity V_j which places the (v.i.) at position 4 at the virtual base circle and at i on the leading profile of the trailing tooth as shown in Fig. 2

It is now necessary to involve the gear tooth geometry. The solution will involve the assumption

$$r_i = R_i = R_{or} - d_i$$

where

$$d_i = V_j t_f \cos\alpha \qquad (20)$$

Thus from the geometry of Fig. 2 it can be seen that θ_a can be approximated from:

$$\tan\theta_a = \frac{V_j t_f \sin\alpha}{R_{or} - V_j t_f \cos\alpha} = \frac{d_i \tan\alpha}{R_{or} - d_i} = \frac{(R_{or} - R_i)\tan\alpha}{R_i} \qquad (21)$$

However, we cannot use d_i to calculate θ_a except as an approximation because the angular origin for θ_a is along the radius vector R_x (Fig. 3) passing through the time origin at "0" while d_i is measured along the R_i radius vector terminating at point "i" on the leading profile of the trailing tooth, which is the terminating vector position for the angle θ_a; thus (see Fig. 3):

$$R_x = R_i \cos\theta_a = (R_{or} - d_i)\cos\theta_a \qquad (22)$$

$d_x = R_{or} - R_x = R_{or} - (R_{or} - d_i)\cos\theta_a$ (See Fig. 3)
Noting that:

$$d_x \tan\alpha = R_x \tan\theta_a \qquad (23)$$

it can be shown that:

$$d_x = R_{or}\cos\alpha - [(R_{or}\cos\alpha)^2 - d_i(2R_{or} - d_i)]^{1/2}\cos\alpha. \qquad (24)$$

so that, $\theta_a = \tan^{-1}[d_x \tan\alpha/(R_{or} - d_x)]$.

Then as a check on the calculated value of d_x above:

$$d_i = R_{or} - \frac{R_{or} - d_x}{\cos\theta_a} \qquad (25)$$

which should be the same as before.

If it is noted that $R_i = R_{or} - d_i$ then (see Fig. 2).

$$\theta_i = \text{inv}\,\phi_i = \tan\phi_i - \phi_i = \left[\left(\frac{R_i}{R_b}\right)^2 - 1\right]^{1/2} - \cos^{-1}\left(\frac{R_b}{R_i}\right) \qquad (26)$$

Note that ϕ_i is a function of R_i and d_i making an explicit solution for (R_i or d_i) impossible when V_j is specified leaving d_i or R_i as the dependent variable. Also.

$$\theta_r = \frac{\pi}{N} - \frac{4\Delta a \tan\phi_n}{R} - 2\theta_n \qquad (27)$$

where: $\theta_n = \text{inv}\,\phi_n = \tan\phi_n - \phi_n$ for spur gears and $\theta_r = \pi/n - 2\Delta a \tan\phi_t/R_t - 2\theta_t$ for helical gears

where

$\theta_t = \text{inv}\,\phi_t = \tan\phi_t - \phi_t$ and $\tan\phi_t = \tan\phi_n \sec\psi$

$$\text{and} \quad R_t = \frac{N}{2P_t} \qquad (28)$$

Further

$$\theta_o = \tan\phi_o - \phi_o = \left[\left(\frac{R_{or}}{R_b}\right)^2 - 1\right] - \cos^{-1}\left(\frac{R_b}{R_{or}}\right) \qquad (29)$$

Now the gear angle of rotation, θw, between points 1 and i in Fig. 2, can be calculated from

$$\theta_w = \theta_o + \theta_r + \theta_i + \theta_a \qquad (30)$$

so that

$$t_w = \frac{\theta_w}{\omega_g} = \frac{30(\theta_o + \theta_r + \theta_i + \theta_a)}{\pi n} \quad \text{sec} \qquad (31)$$

where

$$n = \text{rev./min}$$

It is now possible to equate the time of flight t_f of the oil jet to the time of gear rotation t_w, so that

$$t_w(\text{g.t.}) = \frac{30\theta_w}{\pi n} = \frac{d_i}{(V_j \cos \alpha)} = t_f(\text{v.i.}) \qquad (32)$$

Since θ_i is $fn(d_i)$, the impingement depth cannot be solved explicitly but must be iterated numerically. Thus, we solve for V_j so that an explicit solution is possible as follows:

$$V_j = \frac{\pi d_i n}{30\theta_w \cos \alpha} = \frac{d_i \omega_g}{\theta_w \cos \alpha} \qquad (33)$$

It would be desirable to graph the results of these formulas as in Figs. 4 and 5. Thus the independent variables will be normalized to provide dimensionless solutions to the above results. The principle parameters used are V_j and d_i so that we will express them in terms of the dimensionless parameters ν_j, δ_i and N as:

$$\nu_j = \frac{V_j}{V_g} = \frac{V_j}{\omega_g R_{or}} = \frac{d_i}{\theta_w R_{or} \cos \alpha} \qquad (34)$$

and

$$V_j = \nu_j \omega_g R_{or} \delta_i = \frac{d_i}{W.D.} = \frac{d_i}{2/P_n} = \frac{d_i P_n}{2} \quad \text{and} \quad d_i = \frac{2\delta_i}{P_n} \qquad (35)$$

where W.D. is the whole depth.

Thus the time of flight (t_f) from the trailing edge of the leading tooth top land at radius R_{or} to the radius of impingement R_i on the leading profile of the trailing tooth is:

$$t_f = \frac{2\delta_i}{\nu_j \omega_g P_n R_{or} \cos \alpha} \qquad (36)$$

and in terms of N, using $R_{or} = (N + 2 \cos \psi + 2\Delta n)/(2P_n \cos \psi)$:

$$t_f = \frac{4\delta_i \cos \psi}{[\nu_j \omega_g (N + 2 \cos \psi + 2\Delta N) \cos \alpha]} \qquad (37)$$

Then the time of rotation t_w from the trailing edge of the leading tooth top land at radius R_{or} to to the jet line when it intercepts the impingement point at radius R_{or} on the leading profile of the trailing tooth is:

$$t_w = \frac{\theta_w}{\omega_g} \qquad (38)$$

where

$$\theta_w = \theta_o + \theta_r + \theta_i + \theta_a \qquad (39)$$

so that angular geometry expressed in fundamental terms of N, ΔN, ϕ, ψ, α and δ_i or ν_j are; starting with the vertorial angle θ_a (see Fig. 1) is:

$$\tan \theta_a = d_i \tan \frac{\alpha}{R_i}, \text{ so that}$$

$$\theta_a = \tan^{-1} \left[\frac{4\delta_i \tan \alpha \cos \psi}{N + 2 \cos \psi + 2\Delta N - 4\delta_i \cos \psi} \right] \qquad (40)$$

Next the impingement angle θ_i (see Fig. 1) is:

$$\theta_i = \tan \phi_i - \phi_i = \left(\frac{\rho_i^2}{\rho_b^2} - 1 \right)^{1/2} - \cos^{-1} \left(\frac{\rho_b}{\rho_i} \right) \qquad (41)$$

where

$$\rho_i = 1 - \frac{4\delta_i \cos \psi}{N + 2\Delta N + 2 \cos \psi}$$

$$\rho_b = \frac{N \cos \phi_t}{N + 2\Delta N + 2 \cos \psi}$$

thus

$$\left(\frac{\rho_i}{\rho_b} \right) = \frac{((N + 2 \cos \psi + 2\Delta N) - 4\delta_i \cos \psi)}{N \cos \phi_t} \qquad (42)$$

and

$$\rho_{or} = 1$$

Now this is valid only when (N is given):

$$\delta_i \leq \frac{N + 2\Delta N + 2 \cos \psi - N \cos \phi_t}{4 \cos \psi} = \delta_i(\max) \qquad (43)$$

or when δ_i is given

$$N \geq 2 \left[\frac{(2\delta_i - 1) \cos \psi - \Delta N}{1 - \cos \phi_t} \right] = N(\min) \qquad (44)$$

the tooth space angle θ_r at the base diameter is

$$\theta_r = \frac{\pi}{N} - \frac{4\Delta N}{N} \tan \phi_t - 2\theta_t \qquad (45)$$

where

$$\theta_t = \tan \phi_t - \phi_t - \left[\left(\frac{\rho_t}{\rho_t} \right)^2 - 1 \right]^{1/2} - \cos^{-1} \frac{\rho_b}{\rho_t} \qquad (46)$$

where

$$\rho_t = \frac{N}{N + 2\cos\psi + 2\Delta N}$$

and

$$\frac{\rho_t}{\rho_b} = \frac{1}{\cos\phi_t} = \sec\phi_t$$

and finally the involute angle θ_o to the outside diameter is:

$$\theta_o = \text{inv}\,\phi_{or} = \tan\phi_{or} - \phi_{or} = \left(\frac{1}{\rho_b^2} - 1\right)^{1/2} - \cos^{-1}(\rho_b) \tag{47}$$

again it is possible to equate the times of flight t_f and rotation t_w, now in terms of dimensionless parameters, so that

$$\frac{\theta_w}{\omega_g} = \left[\frac{4\,\delta_i\cos\psi}{\nu_j(N + 2\cos\psi + 2\Delta N)\cos\alpha}\right] \tag{48}$$

Therefore, if the dimensionless depth $\delta_i \leq \delta_i$ (max) is given the dimensionless velocity is calculated from:

$$\nu_j = \left[\frac{4\delta_i\cos\psi}{\theta_w(N + 2\cos\psi + 2\Delta N)\cos\alpha}\right] \tag{49}$$

Also, if the dimensionless velocity ν_j is given then the dimensionless depth δ_i is:

$$\delta_i = \frac{\theta_w\nu_j(N + 2\cos\psi + 2\Delta N)\cos\alpha}{4\cos\psi} \tag{50}$$

where the limits for δ_i and/or N from Eqs. 43 and 44 must be observed.

Further, solving for δ_i must be done by an iteration technique since $\theta_w(\delta_i)$ is a function of δ_i and is therefore not explicit.

RESULTS OF COMPUTERIZED PARAMETRIC STUDIES

As noted in the introduction a completely new analytical approach has been taken to development of the mathematical model for what we identify as the Kinematic model.

The effect of inclination angle (α) in the Kinematic model is shown in Fig. 4 which is in keeping with the physics of the problem. It should be noted here that windage has been neglected in keeping with the results from previous studies (Akin, 1975).

It should also be noted that when fan jets are used and are oriented with the fan perpendicular or broadside to the direction of flow around the gear, the resulting impingement depth will probably compare better with a curve for a slighly larger inclination angle than indicated by the pointing direction of the jet nozzle. Also the effect of jet velocity on depth δ_i is shown in Fig. 5. The curve presented here is for a specific gear design: pressure angle $\phi = 20°$, number of teeth $N = 28$, inclination angle $\alpha = 47°$ and dimensionless jet velocity $V_j/V_g = \nu_j = 0.6468$.

Figure 6 (Akin, 1975) shows the theoretical results compared with the experimental data gathered in 1974. The experimental data did lie substantially below the prediction from the mathematical models at low oil pressures. It is assumed, as also mentioned earlier, that this is the result of (1) the windage effect on a fan-jet at low jet velocity and (2) pressure loss in the nozzle. As the jet velocity is increased the experimental data approaches the curves. The windage study conducted in Akin (1975) involved predicting the trajectory of the oil droplets after they passed into the tooth space between the gear teeth. Under these circumstances the windage affect is considered negligible except for small droplet sizes around 0.001 cm (0.0004 in.).

CONCLUSION

This paper develops the mathematical relations for the "Virtual Kinematic Model" as an improvement over the vectorial model developed earlier. The model solution described herein provides the most energy efficient means of cooling gears-that is, it requires the least pressure or pumping power to distribute the coolant on the tooth surface. Further this nozzle orientation allows impingement to the root if needed and provides the most control when compared to the into-mesh or out-of-mesh cooling.

REFERENCES

Akin, L.S. and Mross, J.J., 1975, "Theory for the Effect of Windage on the Lubricant Flow in the Tooth Spaces of Spur Gears," Journal of Engineering for Industry, Vol. 97, No. 4, pp. 1266-1273.

Akin, L.S. and Townsend, D.P., 1983, "Into Mesh Lubrication of Spur Gears with Arbitrary Offset Oil Jet. Part 1: For Jet Velocity Less Than or Equal to Gear Velocity," Journal of Mechanisms, Transmissions, and Automation in Design, Vol. 105, No. 4, pp. 713-718.

Akin, L.S. and Townsend, D.P., 1983, "Into Mesh Lubrication of Spur Gears with Arbitrary Offset Oil Jet. Part 2: For Jet Velocities Equal to or Greater than Gear Velocity," Journal of Mechanisms, Transmissions, and Automation in Design, Vol. 105, No. 4, pp. 719-724.

Akin, L.S. and Townsend, D.P., 1985, "Lubricant Jet Flow Phenomena in Spur and Helical Gears with Modified Center Distances and/or Addendums - For Out-of-Mesh Conditions," Journal of Mechanisms, Transmissions, and Automation in Design, Vol. 107, No. 1, pp. 24-30.

Akin, L.S., Townsend, D.P., and Mross, J.J., 1975, "Study of Lubricant Jet Flow Phenomena in Spur Gears," Journal of Lubrication Technology, Vol. 97, No. 2, pp. 283-288,295.

Townsend, D.P. and Akin, L.S., 1981, "Analytical and Experimental Spur Gears Tooth Temperature as Affected by Operating Variables," Journal of Mechanical Design, Vol. 103, No. 4, pp. 219-226.

Vogel, W.F., 1945, Involutometry and Trigonometry, Michigan Tool Co., Detroit, MI.

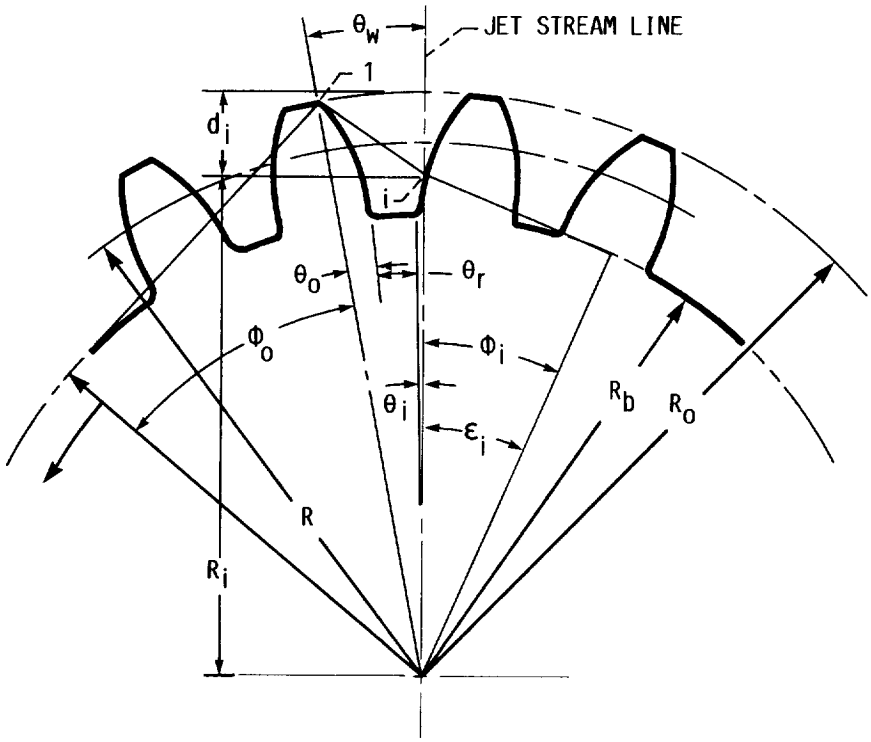

FIGURE 1. - KINEMATIC MODEL WITH RADIAL JET.

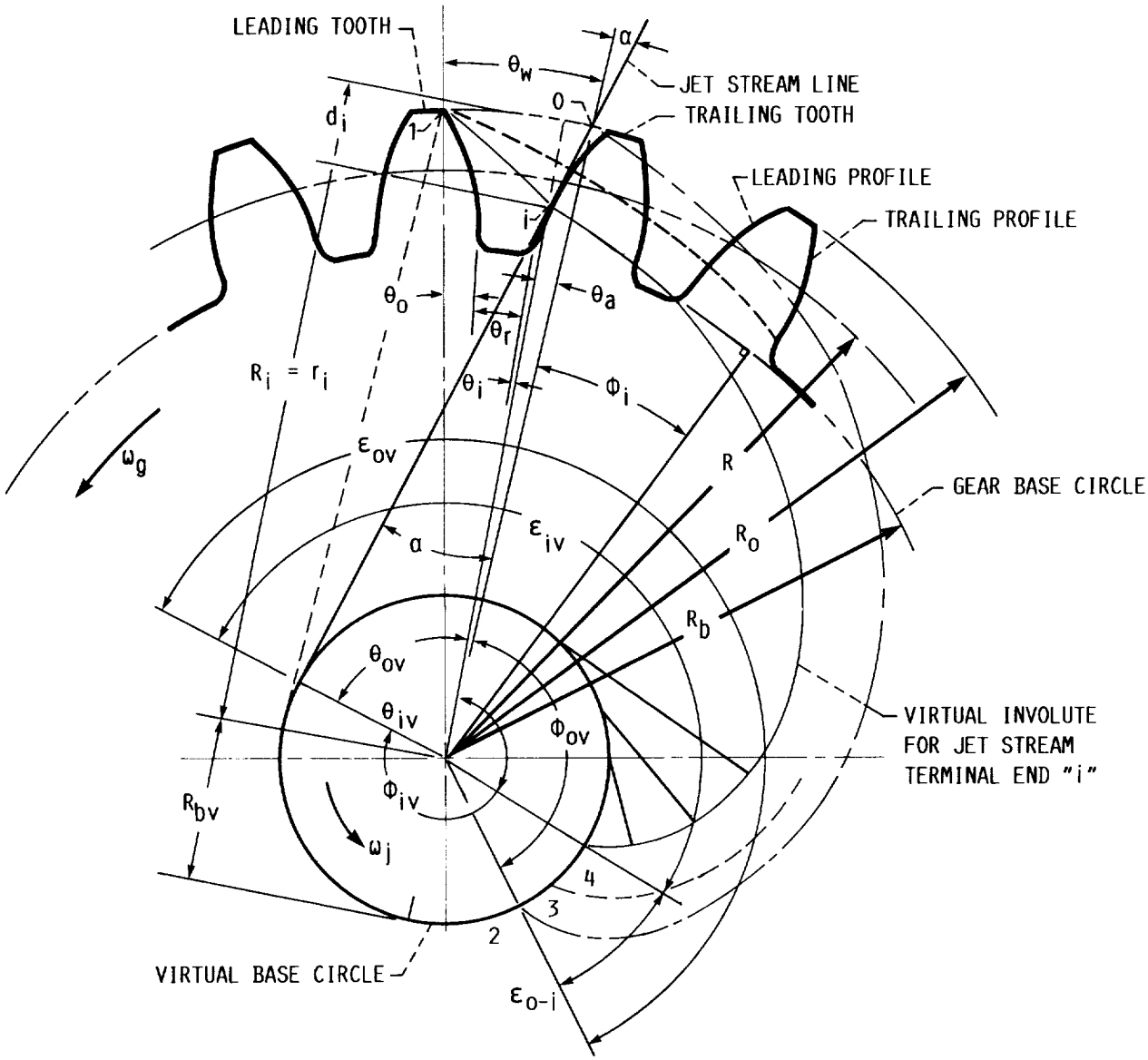

FIGURE 2. - KINEMATIC MODEL WITH ARBITRARY INCLINATION ANGLE "α".

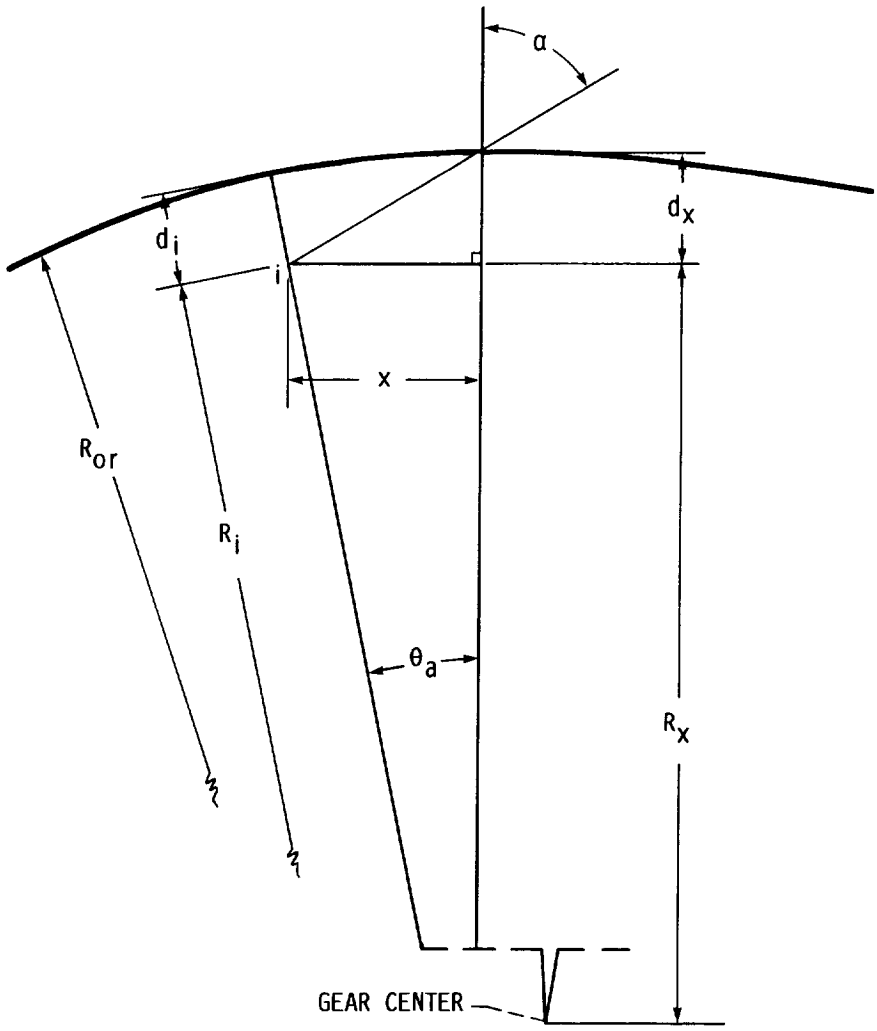

FIGURE 3. - ENLARGED DETAIL OF KINEMATIC MODEL TO SHOW GEOMETRY CORRECTION FOR d_i AS A RESULT OF θ_a.

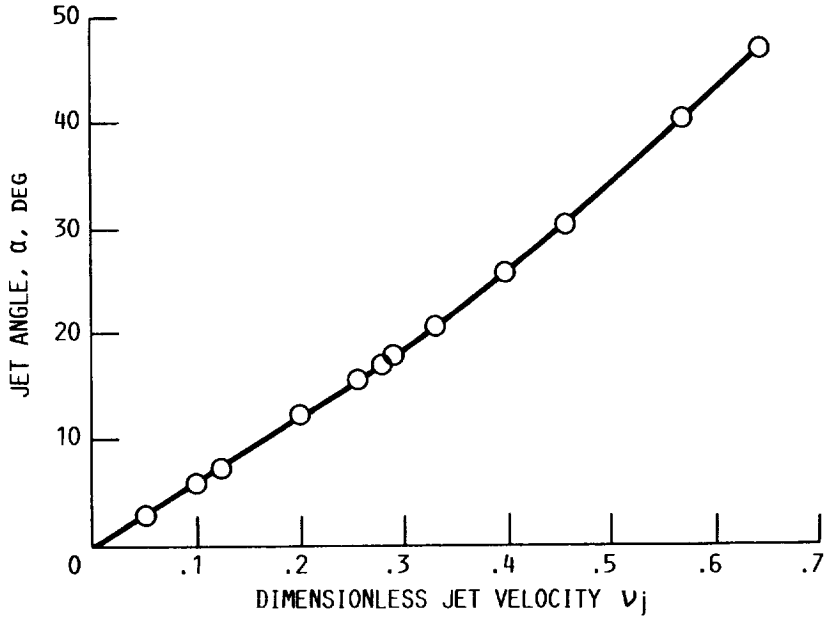

FIGURE 4. - JET ANGLE α WHICH GIVES MAXIMUM DIMENSIONLESS DEPTH OF IMPINGEMENT δ_j FOR A GIVEN DIMENSIONLESS JET VELOCITY ν_j.

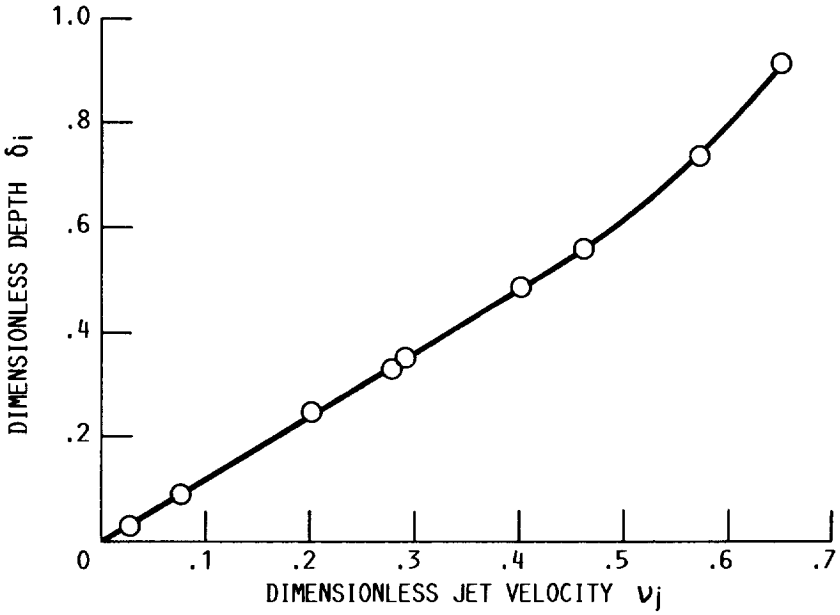

FIGURE 5. - DIMENSIONLESS δ_i FOR A GIVEN DIMENSIONLESS JET VELOCITY ν_j (AT OPTIMUM VALUE FOR ALPHA) $\alpha = 47^0$, PRESSURE ANGLE, 20^0; NUMBER OF TEETH, 28; 8 DIAMETRIAL PITCH.

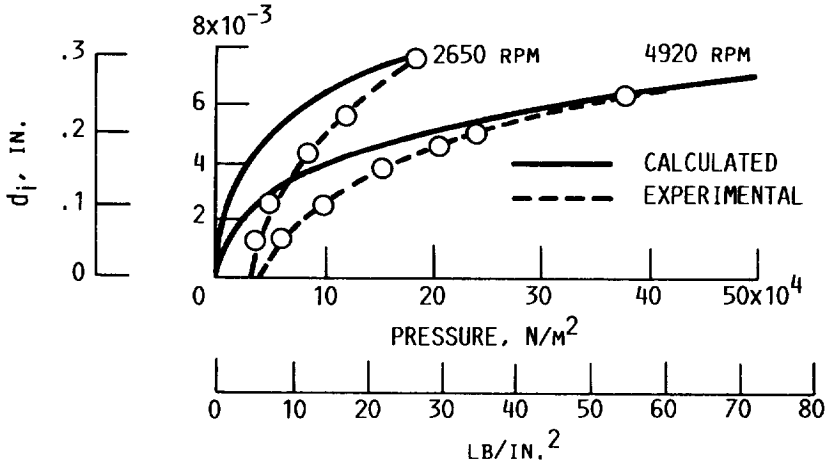

FIGURE 6. - CALCULATED AND EXPERIMENTAL IMPINGEMENT DEPTH VERSUS OIL JET PRESSURE AT 4920 AND 2560 RPM.

NASA
National Aeronautics and Space Administration

Report Documentation Page

1. Report No.	2. Government Accession No.	3. Recipient's Catalog No.
NASA TM-101460 AVSCOM TR-88-C-034		

4. Title and Subtitle

Lubricant Jet Flow Phenomena in Spur and Helical Gears with Modified Addendums—for Radially Directed Individual Jets

5. Report Date

6. Performing Organization Code

7. Author(s)

Lee S. Akin and Dennis P. Townsend

8. Performing Organization Report No.

E-4533

9. Performing Organization Name and Address

NASA Lewis Research Center
Cleveland, Ohio 44135-3191
and
Propulsion Directorate
U.S. Army Aviation Research and Technology Activity—AVSCOM
Cleveland, Ohio 44135-3127

10. Work Unit No.

505-63-51
1L162209A47A

11. Contract or Grant No.

12. Sponsoring Agency Name and Address

National Aeronautics and Space Administration
Washington, D.C. 20546-0001
and
U.S. Army Aviation Systems Command
St. Louis, Mo. 63120-1798

13. Type of Report and Period Covered

Technical Memorandum

14. Sponsoring Agency Code

15. Supplementary Notes

Prepared for the Fifth International Power Transmission and Gearing Conference sponsored by the American Society of Mechanical Engineers, Chicago, Illinois, April 25-27, 1989. Lee S. Akins, California State University, Long Beach, California 90815 (work funded under NASA Grant NAG3-20) and Dennis P. Townsend, NASA Lewis Research Center.

16. Abstract

This paper develops the mathematical relations for the "Virtual Kinematic Model" as an improvement over the vectorial model developed earlier. The model solution described herein provides the most energy efficient means of cooling gears—that is, it requires the least pressure or pumping power to distribute the coolant on the tooth surface. Further, this nozzle orientation allows impingement to the root of the tooth if needed and provides the most cooling control when compared to into-mesh or out-of-mesh cooling.

17. Key Words (Suggested by Author(s))	18. Distribution Statement
Lubrication; Gears; Cooling; Oil jet flow; Gear geometry	Unclassified – Unlimited Subject Category 37

19. Security Classif. (of this report)	20. Security Classif. (of this page)	21. No of pages	22. Price*
Unclassified	Unclassified	12	A03

NASA FORM 1626 OCT 86

*For sale by the National Technical Information Service, Springfield, Virginia 22161